

See discussions, stats, and author profiles for this publication at: <https://www.researchgate.net/publication/322421546>

# Radio frequency dielectric properties of limestone and sandstone from Ewekoro, Eastern Dahomey Basin

Article in *Advances in Applied Science Research* · January 2013

CITATIONS

4

READS

39

2 authors, including:



[Olawale Olatinsu](#)

University of Lagos

18 PUBLICATIONS 78 CITATIONS

[SEE PROFILE](#)

Some of the authors of this publication are also working on these related projects:



Reservoir Characterization [View project](#)



Rock Properties [View project](#)

## **Radio frequency dielectric properties of limestone and sandstone from Ewekoro, Eastern Dahomey Basin**

<sup>1</sup>Olatinsu O. B., <sup>1</sup>Olorode D. O. and <sup>2</sup>Oyedele K. F.

<sup>1</sup>Department of Physics, Faculty of Science, University of Lagos, Lagos, Nigeria

<sup>2</sup>Department of Geosciences, Faculty of Science, University of Lagos, Lagos, Nigeria

---

### **ABSTRACT**

*The dielectric properties of nine rock samples [limestone (8) and sandstone (4)] collected from Ewekoro in Ogun State, Nigeria were studied in the range 10 kHz – 110 MHz under ambient atmospheric conditions. It is found that dielectric constant ( $\epsilon'_r$ ) values of the dry samples decreases with increase in frequency in the range of measurement. Dielectric dispersion is relatively large in almost all the samples. Conductivity dispersions followed the opposite trend increasing in values with increase in frequency. Peaks are more pronounced in loss tangent (D) curve than in dielectric loss ( $\epsilon''_r$ ) curve. This is an indication that overall electrical response of these samples is better revealed by loss tangent variation than dielectric loss variation. All the studied samples are governed by Cole-Cole dispersion which indicates a distribution of relaxation times which is common for multicomponent systems. This is confirmed by the value of the spread parameter which is below 0.5 for all the samples.*

**Keywords:** Dielectric dispersion, relaxation frequency, limestone, sandstone.

---

### **INTRODUCTION**

High-frequency electromagnetic waves travel in the ground in analogous manner to seismic waves. Instead of being determined by the elastic parameters the propagation of radar signals is dependent on the dielectric properties of the subsurface rocks. Ground penetrating radar (GPR) is a high resolution, near surface, geophysical method that can be employed to image geological structures and materials in the subsurface (Rust *et al.*, 1999). Successful delineation of subsurface targets using radar depends on electrical conductivity, dielectric constant and magnetic permeability. However, most geological materials are generally assumed to be non-magnetic and as a result their magnetic permeability is negligible (Ngwenya and Sefara, 2009). The generation of radar signal reflection is dependent on the significant differences in relative dielectric constant between rock formations. Knowledge of the electrical properties of rocks in combination with the radar system is important for predicting the performance of radar in geological settings.

Several electrical/dielectric tools have been employed in the investigation of rock properties. The efficient use of these tools depends on the understanding of the mechanisms of dielectric behaviour of rocks (Knight, 1984a, b; Knight and Nur, 1987a, b; Garrouch and Sharma, 1998; Garrouch, 1999). In this present study, dielectric properties of limestone and sandstone samples from Ewekoro have been reported in the frequency range 10 kHz to 110 MHz. The purpose of this study is to understand the complex dielectric dispersion and electrochemical polarization behaviour of these rock types of different chemical composition in support of radar investigation.

## MATERIALS AND METHODS

### 2.1 Materials

Samples of limestone (LM1 – LM5) and sandstone (SA1 – SA4) were obtained from Ewekoro in Ogun State, Nigeria. The samples along with their physical characteristics and chemical compositions are presented in Table 1 and Table 2 respectively.

**Table 1: Physical characteristics of limestone and sandstone of Ewekoro**

Rock type	Colour	Texture
Limestone	Chalk white/light grey/grey/greenish.	Fine coarse grains.
Sandstone	Brown/reddish brown.	Medium coarse grains.

**Table 2: Chemical composition of limestone and sandstone of Ewekoro**

Sample	Proportion of Elemental Oxides (ppm)									
	SiO <sub>2</sub>	Al <sub>2</sub> O <sub>3</sub>	Fe <sub>2</sub> O <sub>3</sub>	TiO <sub>2</sub>	CaO	P <sub>2</sub> O <sub>5</sub>	K <sub>2</sub> O	MnO	MgO	Na <sub>2</sub> O
LM1	3.76	1.07	0.12	-	53.35	-	0.18	0.01	0.28	0.16
LM2	2.69	0.56	0.24	-	54.64	-	0.12	0.01	1.20	0.14
LM3	2.66	0.46	0.16	-	54.86	-	0.12	-	0.24	0.16
LM4	0.79	0.60	0.40	-	55.97	-	0.14	-	0.32	0.16
LM5	3.64	0.82	1.90	-	55.21	-	0.18	-	0.36	0.18
SA1	57.95	28.06	4.74	1.12	1.51	0.03	0.80	0.06	4.13	0.79
SA2	5.54	26.06	4.72	1.17	1.54	0.02	0.91	0.07	4.40	0.91
SA3	59.38	27.06	4.11	1.15	1.58	0.02	0.93	0.06	4.83	0.85
SA4	58.53	27.93	4.27	1.10	1.54	0.03	0.93	0.06	4.68	0.90

LM= limestone; SA=sandstone

### 2.2 Sample preparation for dielectric measurements

Preliminary sample preparation involved cutting the samples into approximately disc shape with the aid of a diamond saw electrically operated through a Siemens angle cutter. A range of sizes in diameter and thickness were obtained, depending on the size of the original lump of sample. The disk-shaped sample surfaces were later ground and polished using grinding machine to obtain as nearly as possible smooth, parallel faces. Sandstone samples due to porosity/pore spaces generally retained some very small degree of roughness. They were then kept in polyethylene bags and later glass containers to avoid absorbing moisture.

### 2.3 Dielectric measurements

In this study, dielectric permittivity and conductivity measurements were carried out on dry samples of limestone and sandstone in the frequency range of the applied field was from 10 kHz to 110 MHz. The dielectric measuring system consisted of a Precision Impedance Analyzer (Agilent 4294) and a test/measurement probe (steel electrode) specially fabricated for parallel plate measurement at the Petrophysics Laboratory of the CSIRO Earth Science and Resource Engineering (CESRE) Unit of the Australian Resources Research Center, Kensington, Western Australia.

The output parameters from the analyzer are the parallel capacitance  $C_p$  and the parallel resistance  $R_p$ , from which both the real part of the relative dielectric permittivity (dielectric constant)  $\epsilon'_r$  and the conductivity  $\sigma$  from

$$\epsilon'_r(\omega) = \frac{C(\omega)d}{\epsilon_o A} \text{ and } \sigma(\omega) = \frac{d}{R(\omega)A} \text{ respectively. The imaginary relative permittivity (dielectric loss) } \epsilon''_r$$

was obtained using  $\epsilon''_r(\omega) = \frac{\sigma(\omega)}{\omega\epsilon_o}$  or  $\epsilon''_r = \frac{R^{-1}(\omega)d}{\omega\epsilon_o A}$ . Also, the loss tangent  $D$  was computed from the ratio of

$$\epsilon''_r \text{ and } \epsilon'_r \text{ i.e. } D = \frac{\epsilon''_r}{\epsilon'_r}. \text{ Where } d \text{ is the distance between the electrodes, } A \text{ their area; Angular frequency}$$

$\omega = 2\pi f$  and  $\epsilon_o$  is the permittivity of free space. The diameter and thickness of the samples were measured using an electronic digital calliper. Good electromagnetic shielding was implemented to the whole sample holder in order to reduce noise problems that are common, especially at low frequencies. The material was mounted in a sample cell between the parallel circular electrodes thus forming a sample capacitor. The material placed in the capacitor can be

considered as an equivalent electrical circuit which consists of a capacitance,  $C(\omega)$ , in parallel with a resistance,  $R(\omega)$ . These values are the output of the dielectric analyzer.

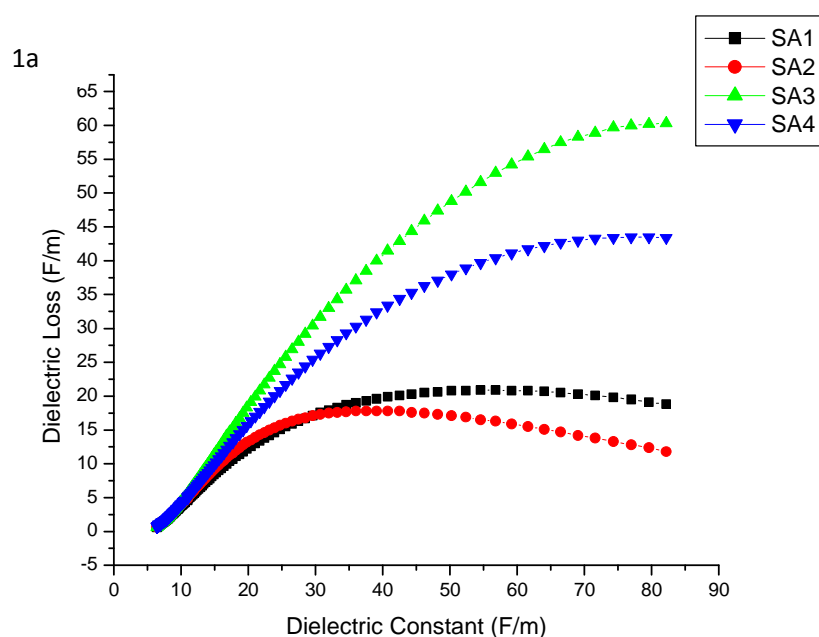
## RESULTS AND DISCUSSION

### 3.1 Cole-Cole Plots

The Cole-Cole plot (Cole-Cole, 1941) was utilized as a quick way of obtaining insights into the polarization and conduction mechanisms in the rocks. The Debye response (Debye, 1929) has frequently been used to describe dielectric dispersion in a system with a single relaxation time. For a Debye-type relaxation process in which a single relaxation time  $\tau$  is assumed, this should produce a semi-circle with center on the horizontal axis. However, many materials, including rocks, deviate from Debye behaviour, suggesting the presence of a distribution of relaxation times. The plots for the rocks in this study are shown in Figures 1a and 1b. It is found that the dielectric dispersion of all the samples is governed by Cole-Cole relaxation behaviour due to orientation polarization process. This type of behaviour has been reported for geologic materials by several workers (Saint-Amant and Strangway, 1970; Knight, 1984a; Knight and Nur 1987a; Sengwa and Soni, 2005, 2008). The Cole-Cole equation for dielectric dispersion is

$$\epsilon^*(\omega) = \epsilon' - i\epsilon'' = \epsilon_\infty + \frac{\epsilon_0 - \epsilon_\infty}{1 + (i\omega\tau)^{1-\alpha}}$$

where  $\epsilon_0$  is the low frequency limiting value of permittivity or static dielectric constant,  $\epsilon_\infty$  the high frequency limiting value of permittivity,  $\omega$  the angular frequency,  $\tau$  the characteristic relaxation time of the dipole relaxation in the system and  $\alpha$  the spread parameter which governs the broadness of the distribution ( $0 < \alpha < 1$ ). The evaluated values of  $\epsilon_0$ ,  $\epsilon_\infty$ , dielectric strength  $\Delta\epsilon = \epsilon_0 - \epsilon_\infty$ , and  $\alpha$  are presented in Table 3. There is significant variation in  $\epsilon_0$  and  $\epsilon_\infty$  for the two sample types.  $\epsilon_0$  varies between 78.51 and 177.71 for sandstone samples while for limestone it varies between 53.11 and 143.30.  $\epsilon_\infty$  for sandstone is in the range 6.41-7.07 while for limestone the range is 5.49-8.33. Table 3 also show that the observed  $\alpha$  values of all the samples are lower than 0.5, which depicts a distribution of relaxations consistent with the multicomponent nature of these samples.



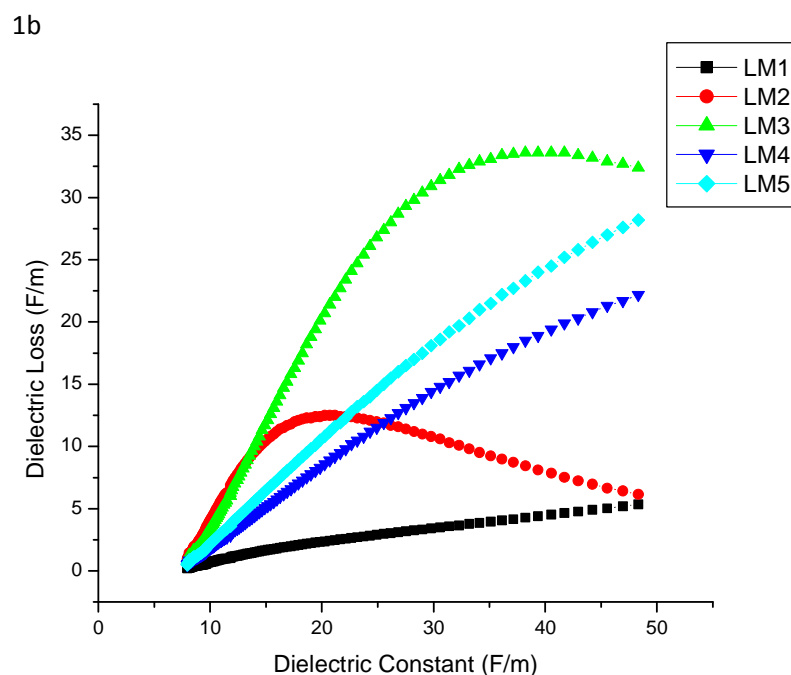


Figure 1: Cole-Cole plots for the rock samples

Table 3: Values of dielectric parameters of limestone and sandstone of Ewekoro

Sample	$\epsilon_0$	$\epsilon_\infty$	$\Delta\epsilon$	$\alpha$
LM1	85.85	5.49	80.36	-
LM2	53.11	7.96	45.15	0.4923
LM3	143.30	8.33	134.97	0.3070
LM4	108.47	8.33	100.14	0.4039
LM5	136.42	8.33	128.09	0.3779
SA1	78.51	6.41	72.10	0.3808
SA2	63.37	5.69	57.68	0.3809
SA3	177.71	7.07	170.64	0.2694
SA4	144.77	6.41	138.36	0.2220

### 3.2 Dielectric dispersion

The calculated permittivity ( $\epsilon'_r$ ) values of dry limestone and sandstone samples as function of frequency are presented in Figures 2a and 2b. These plots reveal dispersion, which is comparatively large in almost all the samples. Table 2 shows the multicomponent nature of these rock samples in which the overall dielectric behaviour of each is governed by contributions from each component having differing  $\epsilon'_r$ . In earth materials, dielectric dispersion is due to polarization in the sample's bulk volume as a result of charge build-up at grain boundaries of the components of the sample (Saint-Amant and Strangway, 1970).

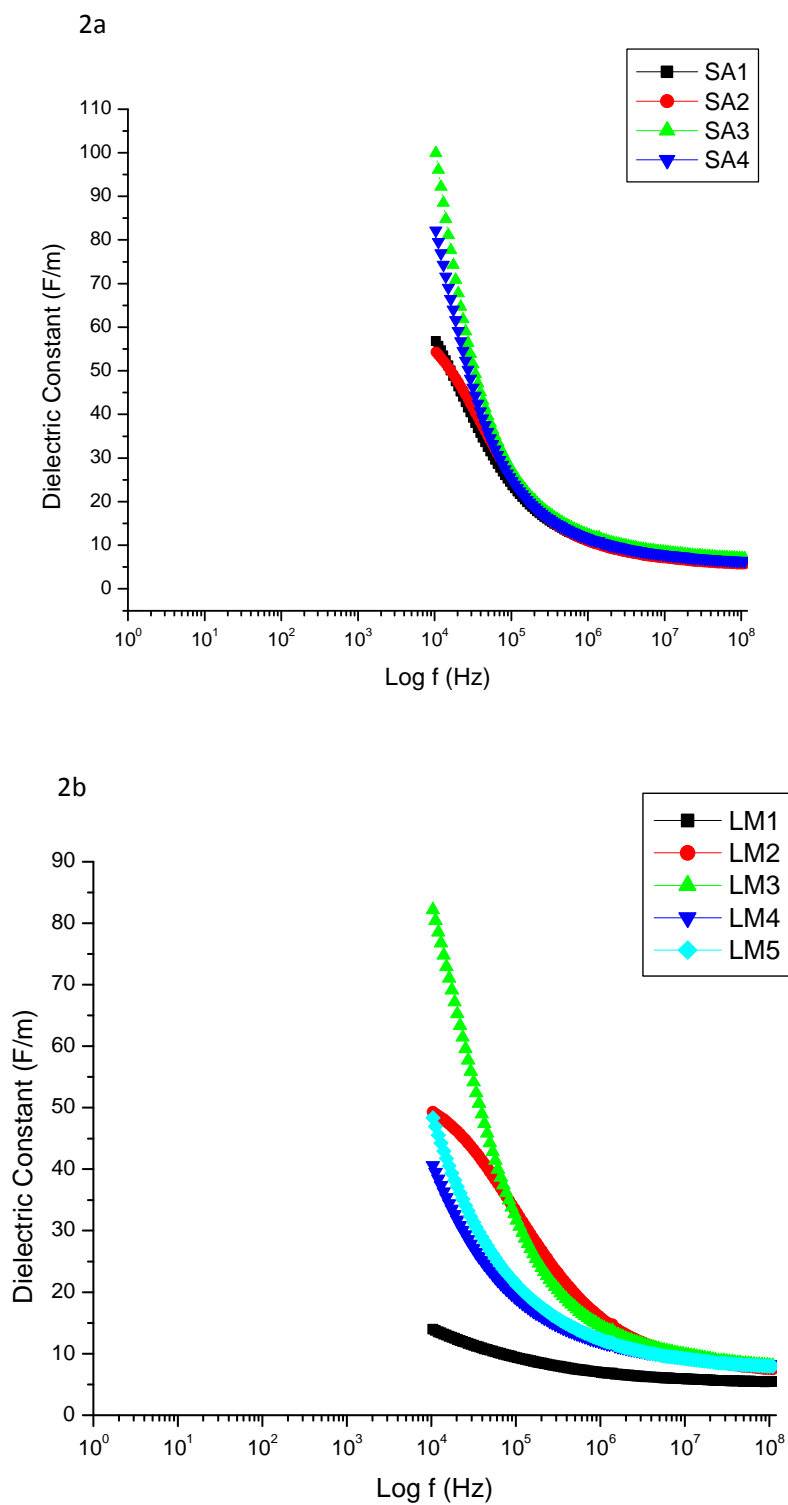


Figure 2: Plots of dielectric constant versus frequency for the rock samples

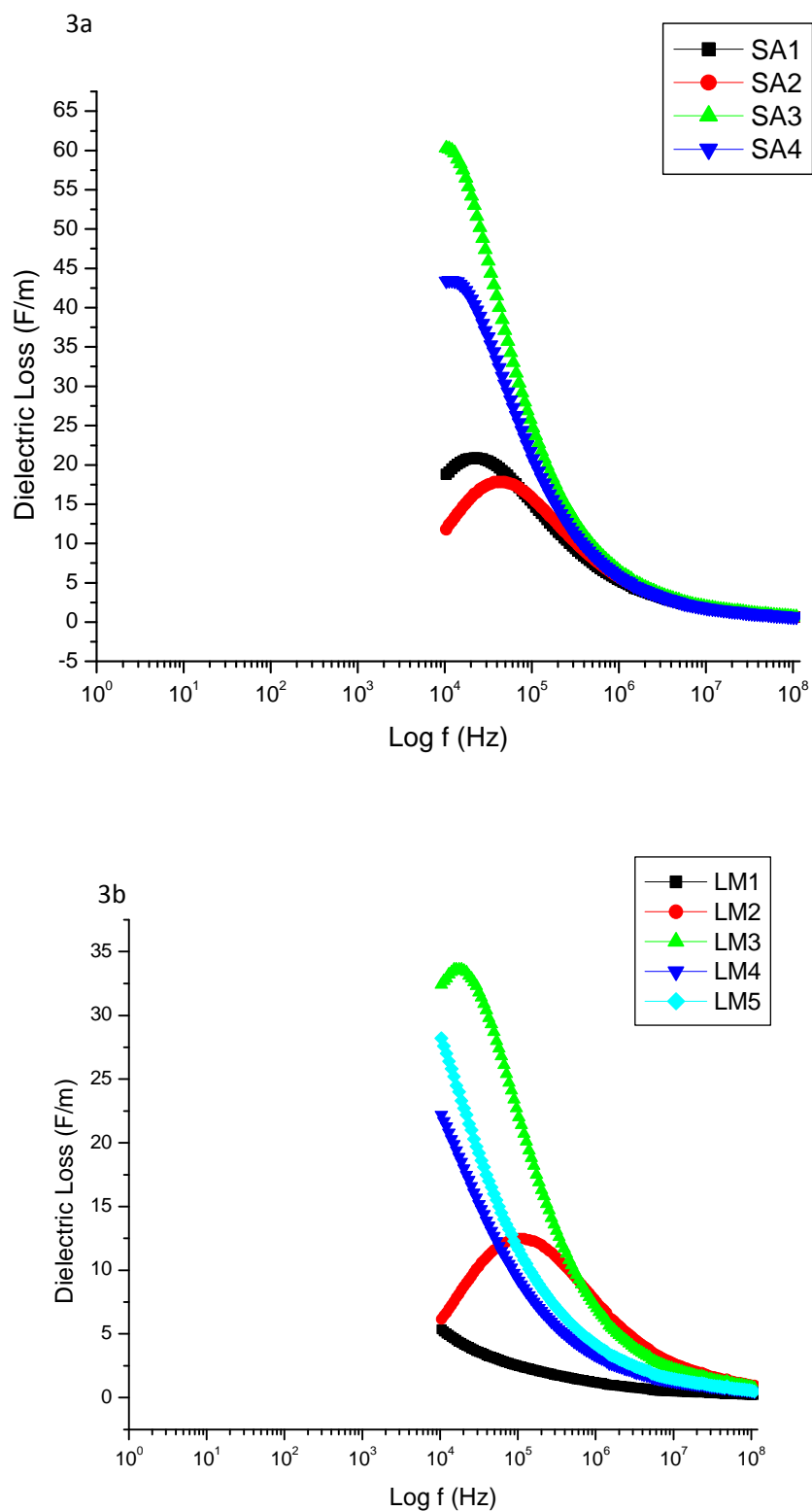


Figure 3: Plots of dielectric loss versus frequency for the rock samples

### 3.3 Dielectric Loss

The imaginary relative permittivity ( $\epsilon_r''$ ) values of the samples are plotted against  $\log f$  in Figures 3a and 3b. SA1, SA2 and SA4 for the sandstone samples show maximum absorption peaks with corresponding relaxation frequency 23.5 kHz, 42.5 kHz and 42.1 kHz respectively. The relaxation frequency for SA3 is probably below 15 kHz. Only two limestone samples, LM2 and LM3 show peaks in dielectric loss and the corresponding relaxation frequency are 57.2 kHz and 11.2 kHz respectively. It is most likely that this frequency for LM1, LM4 and LM5 is below 5 KHz.

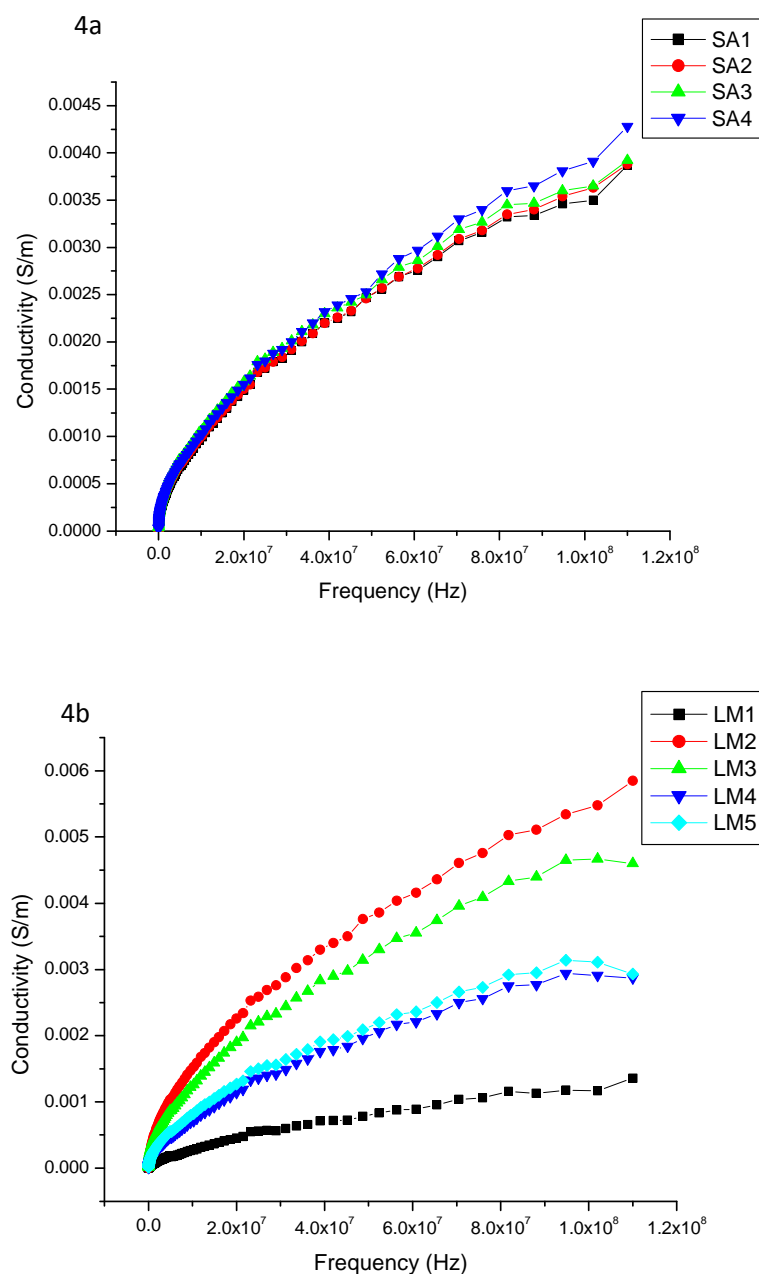


Figure 4: Plots of conductivity against frequency for the rock samples



### 3.4 Conductivity

Figures 4a and 4b show the variation of A.C. conductivity of the studied samples. These all show increase in conductivity with frequency. This is in contrast to dielectric dispersion which is more strongly dependent on frequency, starting with high values at low frequencies and decreasing to asymptotic values at high frequencies. These characteristics have been interpreted as being caused by geometric or textural heterogeneities in the rock system (Sen, 1981; Sen and Chew, 1983). The similar proportion of elemental oxide composition (Table 2) account for the closeness in conductivity values for the sandstone samples. This trend is also observed in the limestone samples except for LM1 with comparatively lower conductivity values.

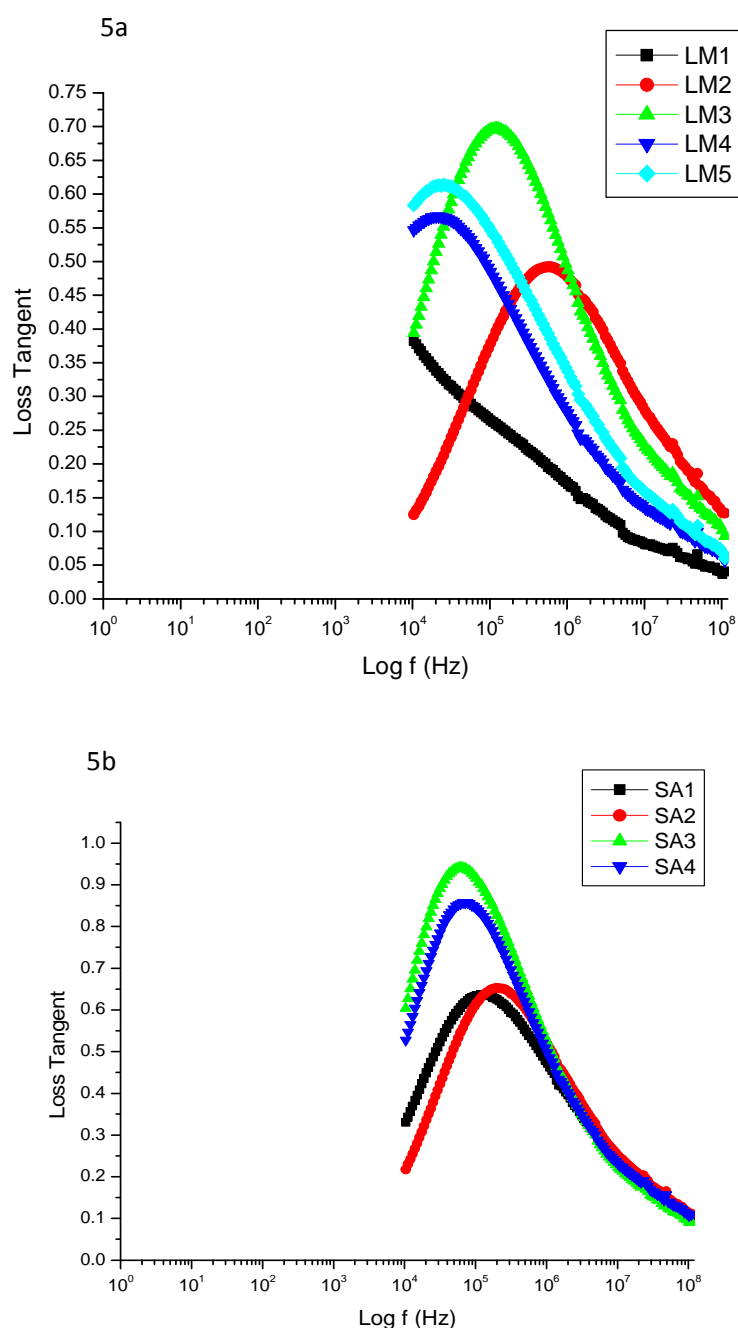


Figure 5: Plots of loss tangent against frequency for the rock samples

### 3.5 Loss Tangent

The variation of loss tangent values with frequency for the samples is shown in Figure 5a and 5b. Loss tangent peaks are more pronounced than maximum absorption peaks. This is found for all the samples except for LM1 which is low probably less than 1 kHz. The critical frequency varies 21.8 kHz to 569 kHz for the other limestone samples while for sandstone the range is between 61.6 kHz and 202 kHz.

### CONCLUSION

The results of this study suggest that sample type and heterogeneity contribute to the dielectric behaviour of rocks. Chemical composition and nature of the two rock types studied clearly distinguish their frequency dependent electrical responses. Similar to other geologic materials all the samples are governed by Cole-Cole relaxation type which means a distribution of relaxation times. The detailed study of the different rocks will assist significantly in radio frequency dielectric technique since radar imaging of the subsurface depends on the average dielectric constant of the rock types available in the area of investigation. Furthermore, the reported values of dielectric parameters and their interpretation can be applied to investigate the various existing frequency dependent empirical dielectric dispersion models of earth materials. These empirical models are often used to model and interpret induced polarization and ground-penetrating radar data.

### Acknowledgements

The authors wish to express their gratitude to CSIRO Earth Science and Resource Engineering (CESRE), Western Australia, for training and permission to use Agilent 4294A for data acquisition and processing. Our special appreciation goes Dr. Ben Clennell and Dr. Matthew Josh for rendering technical assistance to the first author during his visit to CESRE.

### REFERENCES

- [1] K.S. Cole, R.H. Cole, *J. of Chem Phys*, **1941**, 9, 341-351.
- [2] P. Debye; *Polar Molecules*, Dover Publ., New York, **1929**.
- [3] A.A. Garrouch, M.M. Sharma, *The Log Anal.*, **1998**, 39, 48-53.
- [4] A.A. Garrouch, *The Log Anal.*, **1999**, 40, 271-279.
- [5] R.J. Knight, Ph.D. thesis, Stanford University (US, **1984**).
- [6] R. Knight, *J. Geomagn. Geoelectr.*, **1984**, 35, 767-776.
- [7] R.J. Knight, A. Nur, *Geophysics*, **1987**, 52, 644-654.
- [8] R.J. Knight, A. Nur, *The Log Anal.*, **1987**, 28, 513-519.
- [9] B. Ngwenya, M.T. Mafiri, P.G. Sefara, In: 11<sup>th</sup> SAGA Biennial Technical Meeting and Exhibition (Swaziland, **2009**).
- [10] A.C. Rust, J.K. Russell, R.J. Knight, *J. Vol. geo. res.*, **1999**, 91, 79-96.
- [11] M. Saint-Amant, D.W. Strangway, *Geophysics*, **1970**, 35, 624-645.
- [12] P.N. Sen, *Geophysics*, **1981**, 46, 1714-1720.
- [13] P.N. Sen, W.C. Chew, *J. Microwave and Power*, **1983**, 18(1), 95-105.
- [14] R.J. Sengwa, A. Soni, *Indian J. radio & Space Physics*, **2005**, 43, 777-782.
- [15] R.J. Sengwa, A. Soni, *Indian J. of radio & Space Physics*, **2008**, 37, 57-63.